https://doi.org/10.30799/jnst.242.19050409 J. Nanosci. Tech. - Volume 5 Issue 4 (2019) 776–779

ISSN: 2455-0191

Share Your Innovations through JACS Directory

Journal of Nanoscience and Technology

Visit Journal at http://www.jacsdirectory.com/jnst

Physicochemical Interactions of APTS-$ZnFe_2O_4$ Nanoparticles with Bovine Serum Albumin (BSA): Biomedical Applications

Neelam[1,2], Mahima Kaushik[1,*]

[1]*Nano-bioconjugate Chemistry Lab, Cluster Innovation Centre, New Delhi – 110 007, Delhi, India.*
[2]*Department of Chemistry, University of Delhi, New Delhi – 110 007, Delhi, India.*

ARTICLEDETAILS

Article history:
Received 24 April 2019
Accepted 04 June 2019
Available online 12 June 2019

Keywords:
Spinel Ferrites
$ZnFe_2O_4$ Nanoparticles
BSA Protein
Bionanoconjugates

ABSTRACT

Proteins have complicated three-dimensional structures with multilevel conformations, which can be altered to different extents on interactions with foreign molecules or nanoparticles. Soft protein like bovine serum albumin (BSA) is the most extensively studied proteins, as on surface adsorption BSA generally undergoes conformational reorientation unlike a hard protein lysozyme. BSA whose structure is similar to that of human serum albumin (HSA) is considered to be a model protein. In fact, study of BSA can be considered to be a key step before moving to its human version. Understanding the interaction of these proteins with nanomaterials becomes extremely important for utilizing them in biomedical applications especially in drug delivery and even disease diagnosis. Different types of surface functionalization are being tried on nanoparticle for improving their physicochemical properties. Keeping all these view in mind, this Study was designed to understand the physicochemical properties of 3-aminopropyl triethoxy silane (APTS) coated $ZnFe_2O_4$ nanoparticles upon their interaction with BSA using UV-visible spectroscopy, circular dichroism (CD) spectroscopy and CD melting studies.

1. Introduction

Nanoparticles (NPs) because of their capability to interact with the biomolecules like DNA/ RNA or proteins in fundamental ways have shown enormous potential for biomedical/ nanomedicine applications. In the burgeoning field of nanotechnology, integration of nanotechnology with biology is expected to provide major advances in material science, bio-engineering and molecular diagnostics [1]. Especially, conjugate of nanoparticles with protein have substantial advances in the sensing, assembly, magnetic resonance imaging (MRI) diagnosis, hyperthermia therapy, drug delivery, receptor targeting and imaging. Conjugation of nanoparticles and proteins not only stabilizes the system but also originates biocompatible functionalities into the nanoparticles for further biological interactions [2, 3]. Exposure of proteins on the surface of nanoparticles causes formation of layer called protein corona [4]. Various forces like Van der Waals interactions, H- bonding, and solvation forces play key roles in adsorption process of proteins on NPs [5]. Nanoparticles can only be considered safe and effective if their physiological responses are well understood and controlled [6].

However, in nanoparticles and proteins conjugation, more or less structural changes are seen in proteins at the boundary surface of the nanoparticles in most of the cases and basic understanding is needed before using such complexes in biomedical applications [7]. The resulting changes in function and structure can have extensive effects in bio-conjugate applications, as conjugated proteins conformational changes may lead to loss of biological activities or activation of immune response [8]. In addition, a thorough mapping of conformational changes of proteins may help in identification of optimal conditions for preserving functionality followed by conjugations which directs further applications. In this way, fundamental understanding of proteins conformational behavior in bio-conjugate is of utmost importance for the development of bioconjugated nanomaterials [9].

The immense importance of nanomaterials is their size compatibility with most of biological molecules/ structures where surface or biofunctionalization is the pertinent technique to achieve biocompatibility in metal-based nanoparticles in order to make their use in biomedical applications. Size of nanomaterials may be lower than biomolecules and can conjugate with them by accumulating on their surface via covalent or physical interactions. In order to obtain medical breakthrough in therapy and diagnosis, researchers are seeking to explore the intrinsic properties of magnetic nanoparticles [10]. Major advantage of magnetic nanoparticles is their visualization while acting as magnetic contrast agents for MRI. They release drugs when heated under high frequency magnetic field and produce hyperthermia/ ablation of tissues known as magnetic fluid hyperthermia (MFH) [11].

In particular, oxide-based spinel ferrites are considered to be the promising candidates for MRI and hyperthermia treatment, as iron oxides are well known biocompatible candidates. Isolation, purification and separation of various kinds of proteins/ peptides are used almost everywhere i.e. in all the branches of biotechnologies and biosciences where a very simple magnetic separation can do well [12].

BSA because of being similar to that of HSA is considered as one of the best and simplest proteins to work on, for the better understanding of interactions [13]. Serum albumins, one of the most abundant proteins in blood plasma play a major role in disposition of endogenous/ exogenous compounds present in blood and are responsible for drug deposition and efficacy [6]. These proteins play an important role in transportation of nutrients and drugs through human bodies [14]. BSA is very stable and also has no ill effects on other biochemical reactions. This maintains blood pH and helps in maintaining colloidal osmotic pressure [13]. Being major water-soluble protein constituents of circulatory system, BSA serves numerous physiological functions such as delivery of fatty acids (lipids), porphyrins, bilirubin and steroids, binding, transport etc., [15]. Binding of BSA with drugs/ inorganic materials take place via non-covalent mode for efficient delivery of drug in affected areas of the body. As BSA does not affect other enzymes in the body, it is used as a nutrient in cell and microbial culture. BSA is composed of single polypeptide chain comprising of 583 amino acid residues with molecular weight of 69000 Da and 17 disulfide bonds, where disulfide bridges are responsible for the compactness and helical structure stability of BSA molecule [16]. BSA consists of two tryptophan moieties possessing intrinsic fluorescence; one is Trp-212, which is located within a hydrophobic binding pocket of the protein and another is Trp-134 located on the surface of the molecule, along with phenylalanine and tyrosine [17].

Among various oxide-based spinel ferrites $ZnFe_2O_4$, a monodisperse, stable and superparamagnetic novel system is being used as BSA based

*Corresponding Author:mkaushik@cic.du.ac.in(Mahima Kaushik)

https://doi.org/10.30799/jnst.242.19050409

Cite this Article as: Neelam, Mahima Kaushik, Physicochemical interactions of APTS-$ZnFe_2O_4$ nanoparticles with bovine serum albumin (BSA): Biomedical applications, J. Nanosci. Tech. 5(4) (2019) 776–779.

nanocarrier for a promising nanosystem in biomagnetic applications and to perform theranostic treatment. Albumins are also reported to associate with nano-scale particles, to promote their transportation through the cells. In this work, BSA had been taken as the protein model because of its water-soluble nature required for interactions studies, low cost, ready availability, medicinal importance and unusual ligand binding properties. The interaction studies of APTS coated $ZnFe_2O_4$ nanoparticles were explored using various physicochemical techniques like UV-Visible Spectroscopic Studies, CD spectroscopy and CD melting for understanding the conformational alterations of protein on interaction with nanomaterials.

2. Experimental Methods

2.1 Materials

Fe_3O_4 and ZnO nanoparticles were synthesized in our own lab using hydrothermal method. Ammonium hydroxide (NH_4OH), 25% NH_3 were purchased from Alfa Aesar. APTS, phosphate buffer and BSA were purchased from Sigma Aldrich. All the reagents were of analytical grade. Double distilled water was used for all the experiments.

2.2 Characterization

XRD measurements were used to determine the average crystalline size and purity of the phase. XRD spectrum was recorded on Bruker D8 high resolution X-ray diffractometer using Cu-Kα radiation (λ = 0.1541 nm) by step scan at 40 kV and 30 mA, with scan range (2θ) from 20 to 70 °C. FTIR spectrum was recorded using KBr pellets method on Thermo Scientific spectrometer at ambient conditions within 4000 - 400 cm^{-1} range of wave numbers. FE-SEM images show surface morphology of nanoparticles, by which shape of nanoparticles can be analyzed. FE-SEM measurements can also evaluate size of nanoparticles, whereas elemental composition of nanoparticles can be predicted by EDX spectra. Surface morphology/ elemental composition were analyzed using ZEISS Gemini FE-SEM 500 instrument. Metal grids were being used for the sample preparation and sample was coated by gold prior to analysis. This is the simplest, effective and conventional method used for the characterization of nanoparticles and to study BSA interactions with small ligands like drugs and nanoparticles.

The electronic absorption spectrum was recorded at room temperature on Shimadzu dual beam UV-Visible spectrophotometer (UV-1650 PC) using 1.0 cm path length quartz cuvette from 200-700 nm wavelength in sodium phosphate buffer (pH 7.4). Stock solution of BSA was prepared by dissolving BSA in double distilled water. BSA concentration was measured by UV absorption spectroscopy based on Beer Lambert's law using molar absorption coefficient ε_{280} = 43824 $M^{-1}cm^{-1}$ at 280 nm wavelength. Absorption spectra were recorded first on constant BSA concentration (1.25 μM) and then after varying APTS-$ZnFe_2O_4$ NPs concentration (0-400 μM) in the wavelength range of 200-700 nm.

CD spectra were recorded on JASCO (J-815) spectropolarimeter using quartz cell of 1.0 cm path length from 200-340 nm wavelength. A CD spectrum was first corrected for buffer (sodium phosphate buffer, pH 7.4) signal and then results were recorded as mean residue ellipticity in m.deg at room temperature. CD spectra of BSA alone having constant concentration (1.25 μM) and varying concentration of APTS-$ZnFe_2O_4$ NPs (0 - 400 μM) were recorded in sodium phosphate buffer. CD melting experiments of BSA were carried out on CD spectropolarimeter well equipped with Peltier temperature controller to control the temperature change from 40 °C to 90 °C at 222 nm wavelength.

2.3 Preparation of Stock Solutions of BSA and APTS-$ZnFe_2O_4$ NPs

BSA stock solution was prepared using double distilled water. BSA concentration was calculated by Lambert Beer's law using molar absorption coefficient ε_{280} = 43824 $M^{-1}cm^{-1}$ at 280 nm. APTS-$ZnFe_2O_4$ NPs stock solution of 1 mM was prepared in double distilled water and solution was sonicated for 30 mins to get a colloidally stable solution. Interaction of APTS-$ZnFe_2O_4$ NPs with BSA was recorded using various physicochemical techniques on incubating APTS-$ZnFe_2O_4$ NPs solution (concentration dependent manner) with BSA (fixed 1.25 μM conc.) for around 30 minutes prior to the performing of all experiments.

3. Results and Discussion

3.1 Synthesis of APTS-$ZnFe_2O_4$ Nanoparticles

The $ZnFe_2O_4$ NPs were synthesized using a simple and non-toxic/ environment friendly one-pot hydrothermal autoclave method. 0.1 M Fe_3O_4 nanoparticles and 0.1 M ZnO nanoparticles were dissolved in 30 mL distilled water and solution was stirred to achieve homogeneity. Ammonia solution (25%) (3.7 mL) was added and solution was stirred for another 10 min. The mixture was kept in a sealed Teflon vessel at 140 °C for 5 hours. After completion of reaction, mixture was cooled to room temperature, which was purified with water and ethanol several times to remove unreacted constituents and impurities. Synthesized compound was separated out magnetically. The obtained product was again dissolved in 30 mL of double distilled water with 1 ml of APTS at 90 °C with overnight stirring. The final product was filtered. The obtained black precipitate was dried in a hot air oven at 80 °C for 7-8 hours prior to its further characterization and interaction studies.

3.2 XRD Studies

XRD pattern of APTS-$ZnFe_2O_4$ NPs (Fig. 1) is recorded at room temperature. The average grain size of APTS-$ZnFe_2O_4$ NPs was calculated from the broadening of XRD peak. Based on the major diffraction peak size of nanoparticles was found to be nearly 21 nm as calculated from Debye-Scherrer equation [18]. The XRD pattern was consistent with pure phase of $ZnFe_2O_4$ NPs. Crystal growth of $ZnFe_2O_4$ NPs is quite limited in the presence of APTS.

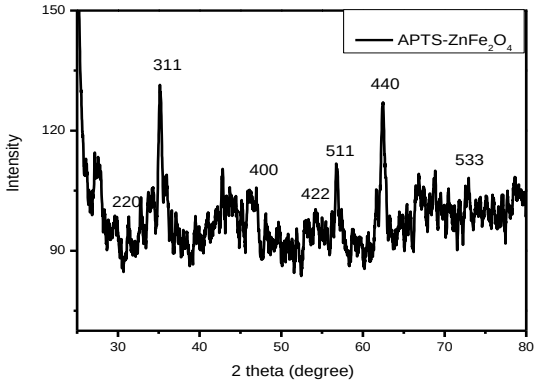

Fig. 1 XRD spectrum of APTS-$ZnFe_2O_4$ NPs

3.3 FTIR Studies

To confirm the surface functionalization of $ZnFe_2O_4$ NPs with APTS, FTIR spectrum was recorded at room temperature and is shown in Fig. 2. The broad band at 1094 cm^{-1} is seen due to the stretching vibrations of Si-O bond and band at 1387 cm^{-1} is due to stretching vibrations of C-N bond. The stronger absorption bands at 3431 cm^{-1} and 1630 cm^{-1} attribute to the introduction of -NH_2 group on the surface of $ZnFe_2O_4$ NPs because of APTS. In addition to these, bands at 566 and 473 cm^{-1} correspond to M-O (M=Fe, Zn) bond stretching frequency. Further, peaks at 2978 cm^{-1} and 2856 cm^{-1} are due to C-H stretching frequency present in the alkyl chain of APTS [19].

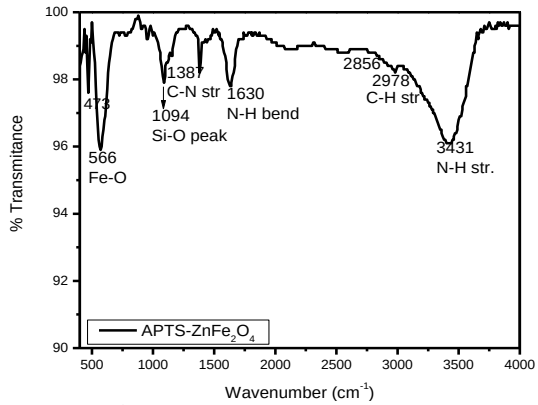

Fig. 2 FTIR spectrum of APTS-$ZnFe_2O_4$ NPs

3.4 FE-SEM and EDX Studies

Surface morphology of APTS-$ZnFe_2O_4$ NPs was analyzed using FE-SEM studies. Particles were found to be nearly spherical but not uniform in shape. The FE-SEM image of nanoparticles is shown in Fig. 3 and its EDX spectrum is shown in Fig. 4. The appearance of characteristic peaks of iron and zinc in EDX spectrum confirm their presence in the nanoparticles. Also, appearance of characteristic peak of silica implies that nanoparticle's surface has been coated with APTS successfully. Further, the peak for gold at around 2.0 (not assigned) in the spectrum appears because the sample was subjected to gold coating prior to FE-SEM analysis.

https://doi.org/10.30799/jnst.242.19050409

Cite this Article as: Neelam, Mahima Kaushik, Physicochemical interactions of APTS-$ZnFe_2O_4$ nanoparticles with bovine serum albumin (BSA): Biomedical applications, J. Nanosci. Tech. 5(4) (2019) 776–779.

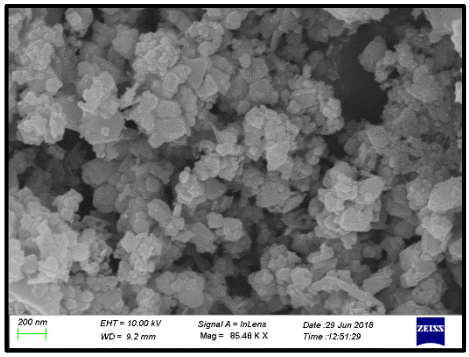

Fig. 3 FESEM image of APTS-$ZnFe_2O_4$ NPs

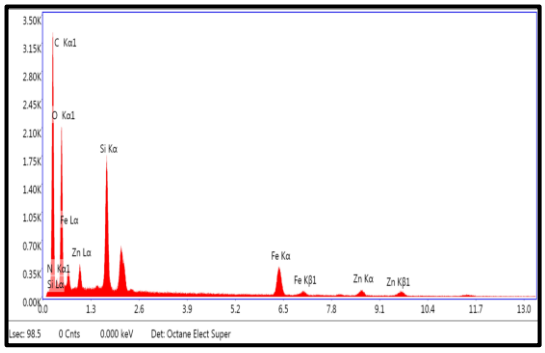

Fig. 4 EDAX image of APTS-$ZnFe_2O_4$ NPs

3.5 UV-Visible Studies

UV-Visible spectrum of as synthesized nanoparticles was recorded and is shown in Fig. 5. The peak at around 446 nm in spectrum of APTS-$ZnFe_2O_4$ NPs signifies the formation of these nanoparticles. The phenomenon of surface plasmon resonance (SPR), which arises due to collective oscillation of free electrons present in conduction band of metals on exposure of electromagnetic radiations [20] is not shown by APTS-$ZnFe_2O_4$ NPs and therefore a sharp peak is not observed in UV-Visible spectrum.

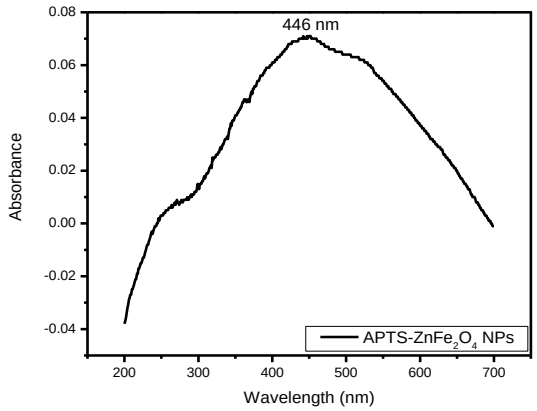

Fig. 5 UV-Visible spectrum of APTS-$ZnFe_2O_4$ NPs

3.6 Interaction Studies of APTS- $ZnFe_2O_4$ NPs with BSA

3.6.1 UV-Visible Spectroscopic Studies

BSA shows a characteristics absorbance band at 280 nm in UV-Visible spectrum. This absorption band corresponds to the π–π* transition of aromatic amino acid residues tyrosine and tryptophan [6]. Absorbance spectra were recorded in sodium phosphate buffer (pH 7.4) on fixed BSA concentration (1.25 µM) and varying APTS-$ZnFe_2O_4$ NPs (0-400 µM) in a concentration dependent manner in wavelength range of 200-700 nm (Fig. 6). Since, isoelectric point of BSA lies in between 4.5 to 4.9, pH of the solution was kept above it, as BSA has sufficient number of negatively charged moieties at this pH and hence can bind with positively surface charged nanoparticles via attractive columbic interactions or electrostatic interactions. The maximum absorbance of BSA at 278 nm gradually increases with increasing concentration of NPs without any peak shift which shows a concentration dependent effect. Similar kind of enhancement in absorbance effect was reported by Kathiravan et al. [21], which revealed that the interaction between BSA and nanoparticles are due to static quenching.

As APTS-$ZnFe_2O_4$ NPs did not show peak at 278 nm, enhancement in absorbance might be due to the alteration in microenvironment of aromatic amino acids (Tyr, Trp) and due to the formation of ground state complex (BSA-APTS-$ZnFe_2O_4$) on interaction of nanoparticles with BSA. Similar results were reported on interaction of BSA with Al_2O_3 NPs [1].

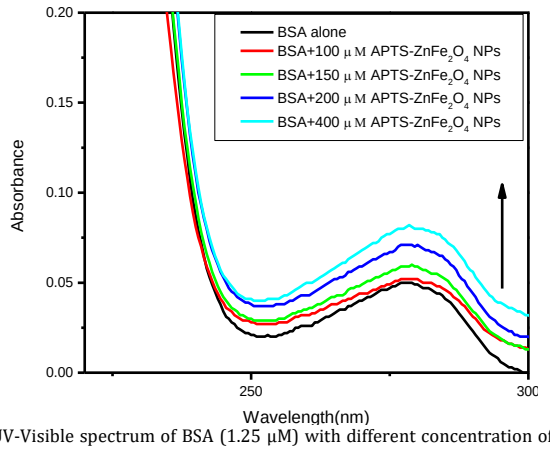

Fig. 6 UV-Visible spectrum of BSA (1.25 µM) with different concentration of APTS-$ZnFe_2O_4$ NPs

3.6.2 Circular Dichroism (CD) Studies

To evaluate the structural changes induced in BSA on interaction with APTS-$ZnFe_2O_4$ NPs Far–UV CD spectroscopy was used. Appearance of characteristics negative peaks at 208 nm and 222 nm in CD spectra of BSA signifies α- helical structure of BSA [22]. Any changes in these peaks indicate conformational changes in the native structure of BSA. A CD spectrum was recorded in absence and presence of different concentrations of APTS-$ZnFe_2O_4$ NPs (50 µM and 100 µM) in sodium phosphate buffer in wavelength range of 200-260 nm as shown in Fig. 7. A decrease in negative ellipticity values of BSA in presence of nanoparticles shows the extent of structural perturbations in α- helical structure of BSA on adsorption with APTS-$ZnFe_2O_4$ NPs. Induced conformational changes in BSA demonstrate strongly the role of size, shape and surface functionalization of nanoparticles [23].

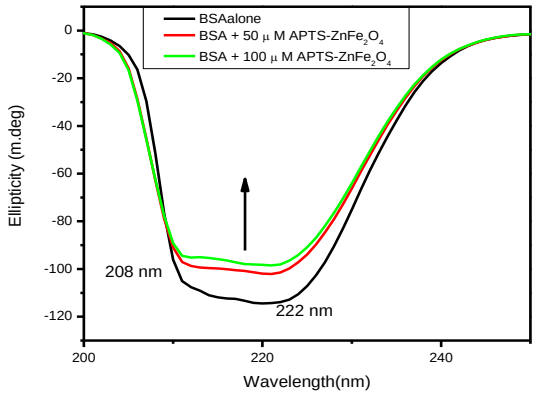

Fig. 7 CD spectra of BSA (1.25 µM) in presence of different concentration of APTS-$ZnFe_2O_4$ NPs

The α-helical content can be evaluated from mean residual ellipticity (MRE) values at 208 nm using the following equation [24],

$$\alpha - Helix\ (\%) = \frac{-MRE_{208} - 4000}{33000 - 4000} \times 100$$

where, 4000 and 33,000 are the MRE of the β-form and random coil conformation cross at 208 nm, and the value of the pure α-helix at 208 nm respectively.

The CD results were presented in terms of (MRE) in deg·cm^2·dmol^{-1} according to the equation given as follows [24],

$$MRE_{208} = \frac{Intensity\ of\ CD(mdeg) at\ 208\ nm}{10\ C_p nl}$$

where, C_p is molar concentration of protein, n is the number of amino acid residues (583 in case of BSA) and l is path length.

For pure BSA, α- helicity was ~51% which decreases to ~46% on addition of APTS-$ZnFe_2O_4$ NPs (50 µM). On further addition of APTS-$ZnFe_2O_4$ NPs (100 µM) further decrease in α- helicity of ~45% was

https://doi.org/10.30799/jnst.242.19050409

Cite this Article as: Neelam, Mahima Kaushik, Physicochemical interactions of APTS-$ZnFe_2O_4$ nanoparticles with bovine serum albumin (BSA): Biomedical applications, J. Nanosci. Tech. 5(4) (2019) 776–779.

observed. This decreases in intensity shows the decrease in α-helical content, which arises because of the binding of APTS-$ZnFe_2O_4$ NPs with amino acid residues of protein. However, shape and peak position in CD spectra indicates that BSA retains its basic structure even after binding with APTS-$ZnFe_2O_4$ NPs.

3.6.3 CD Melting Experiments

Thermal stability of BSA can be quantified on increasing the temperature while recording CD spectrum of BSA. CD melting experiments were performed in order to analyze the relative stability of BSA in presence of APTS-$ZnFe_2O_4$ NPs. Melting temperature was calculated between folded and unfolded state existing in a two-state equilibrium [6]. Fig. 8 shows the CD melting profile of BSA alone and with APTS-$ZnFe_2O_4$ NPs (50 μM). The melting temperature of BSA was found to be 67 °C which changes to 66 °C on conjugation with APTS-$ZnFe_2O_4$ NPs (50 μM). This nominal change in thermal melting was consistent with the findings of other experimental results like UV-Visible spectroscopy and CD data. In case of pure BSA, gradual decrease in ellipticity with increasing temperature indicates loss of secondary structure as a consequence of temperature induced unfolding of protein [25].

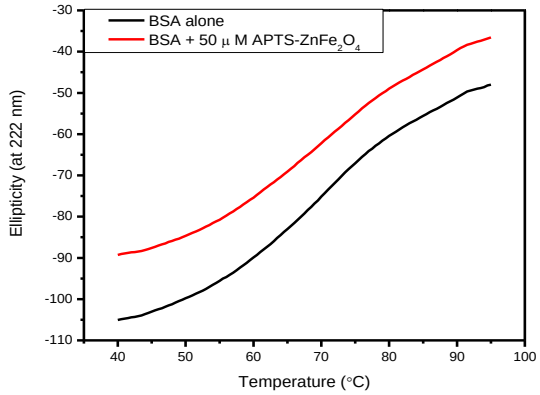

Fig. 8 CD melting spectra of BSA (1.25 μM) alone and in the presence of APTS-$ZnFe_2O_4$ NPs (50 μM)

4. Conclusion

Studying the properties of protein and nanomaterial conjugates is extremely significant as the structural changes or conformation alterations of proteins play functional roles in many cellular processes. Sometimes these alterations may even lead to the loss of biological activities or immune response activation. Keeping this in view, this study intended to explore the effect of surface functionalized nanoparticles on simple protein like BSA. It was observed that the conformation of BSA protein gets altered on an interaction with spinel ferrite APTS-$ZnFe_2O_4$ NPs, which were suggested by the physicochemical techniques like UV-Visible Spectroscopy, CD spectroscopy and CD melting. Studies like this help in facilitating the understanding of protein-nanoparticle conjugates for their future biomedical applications.

Acknowledgement

The author Mahima Kaushik would like to thank Delhi University for its research and development grant. Also, Mahima Kaushik appreciates the constant support from Director, Cluster Innovation Centre and Head, Department of Chemistry, University of Delhi, India.

References

[1] A. Rajeshwari, S. Pakrashi, S. Dalai, V. Iswarya, N. Chandrasekaran, A. Mukherjee, Spectroscopic studies on the interaction of bovine serum albumin with Al_2O_3 nanoparticles, Jour. Lumin. 145 (2014) 859-865.

[2] A. Bhogale, N. Patel, P. Sarpotdar, J. Mariam, P.M. Dongre, A. Miotello, D.C. Kothari, Systematic investigation on the interaction of bovine serum albumin with ZnO nanoparticles using fluorescence spectroscopy, Colloid. Surf. B: Biointerf. 102 (2013) 257-264.

[3] S.V. Bhosale, N.S. Kanhe, S.V. Bhoraskar, S.K. Bhat, R.N. Bulakhe, J.J. Shim, V.L. Mathe, Micro-structural analysis of $NiFe_2O_4$ nanoparticles synthesized by thermal plasma route and its suitability for BSA adsorption, J. Mater. Sci. Mater. Med. 26(8) (2015) 216:1-5.

[4] S.P. Boulos, T.A. Davis, J.A. Yang, S.E. Lohse, A.M. Alkilany, et al., Nanoparticle–protein interactions: a thermodynamic and kinetic study of the adsorption of bovine serum albumin to gold nanoparticle surfaces, Langmuir 29(48) (2013) 14984-14996.

[5] M.A. Jhonsi, A. Kathiravan, R. Renganathan, Spectroscopic studies on the interaction of colloidal capped CdS nanoparticles with bovine serum albumin, Colloid Surf. B: Biointerf. 72(2) (2009) 167-172.

[6] A. Baral, L. Satish, D.P. Das, H. Sahoo, M.K. Ghosh, Construing the interactions between MnO_2 nanoparticle and bovine serum albumin: insight into the structure and stability of a protein–nanoparticle complex, New J. Chem. 41(16) (2017) 8130-8139.

[7] S.D. Medina, S. McDonough, P. Swanglap, C.F. Landes, S. Link, In situ measurement of bovine serum albumin interaction with gold nanospheres, Langmuir 28(24) (2012) 9131-9139.

[8] S. Roy, T.K. Das, Spectroscopic studies of interaction between biologically synthesized silver nanoparticles and bovine serum albumin, J. Nanosci. Nanotechnol. 14(7) (2014) 4899-4905.

[9] A. Bhogale, N. Patel, J. Mariam, P.M. Dongre, A. Miotello, D.C. Kothari, Comprehensive studies on the interaction of copper nanoparticles with bovine serum albumin using various spectroscopies, Colloids Surf. B: Biointerf. 113 (2014) 276-284.

[10] B.K. Paul, K. Bhattacharjee, S. Bose, N. Guchhait, A spectroscopic investigation on the interaction of a magnetic ferrofluid with a model plasma protein: effect on the conformation and activity of the protein, Phys. Chem. Chem. Phys. 14(44) (2012) 15482-15493.

[11] M. Comes Franchini, G. Baldi, D. Bonacchi, D. Gentili, G. Giudetti, et al., Bovine serum albumin-based magnetic nanocarrier for MRI diagnosis and hyperthermic therapy: a potential theranostic approach against cancer, Small 6(3) (2010) 366-370.

[12] I. Safarik, M. Safarikova, Magnetic techniques for the isolation and purification of proteins and peptides, Biomag. Res. Technol. 2(1) (2004) 7:1-17.

[13] S. Ranjan, N. Dasgupta, P. Srivastava, C. Ramalingam, A spectroscopic study on interaction between bovine serum albumin and titanium dioxide nanoparticle synthesized from microwave-assisted hybrid chemical approach, J. Photochem. Photobiol. B: Biol. 161 (2016) 472-481.

[14] B. Pan, D. Cui, P. Xu, Q. Li, T. Huang, et al., Study on interaction between gold nanorod and bovine serum albumin, Colloid Surf. A: Physicochem. Eng. Aspects 295(1-3) (2007) 217-222.

[15] B. Ojha, G. Das, The interaction of 5-(alkoxy) naphthalen-1-amine with bovine serum albumin and its effect on the conformation of protein, J. Phys. Chem. B 114(11) (2010) 3979-3986.

[16] N. Wangoo, C.R. Suri, G. Shekhawat, Interaction of gold nanoparticles with protein: a spectroscopic study to monitor protein conformational changes, Appl. Phys. Lett. 92(13) (2008) 133104:1-3.

[17] A. Ravindran, A. Singh, A.M. Raichur, N. Chandrasekaran, A. Mukherjee, Studies on interaction of colloidal Ag nanoparticles with bovine serum albumin (BSA), Colloid Surf. B: Biointerf. 76(1) (2010) 32-37.

[18] M.D. Carvalho, F. Henriques, L.P. Ferreira, M. Godinho, M.M. Cruz, Iron oxide nanoparticles: the influence of synthesis method and size on composition and magnetic properties, J. Solid State Chem. 201 (2013) 144-152.

[19] R. Rameshbabu, R. Ramesh, S. Kanagesan, A. Karthigeyan, S. Ponnusamy, One pot facile hydrothermal synthesis of superparamagnetic $ZnFe_2O_4$ nanoparticles and their properties, J. Sol-Gel Sci. Technol. 71(1) (2014) 147-151.

[20] Sonia, Komal, S. Kukreti, M. Kaushik, Exploring the DNA damaging potential of chitosan and citrate-reduced gold nanoparticles: Physicochemical approach, Int. J. Biol. Macromol. 115 (2018) 801-810.

[21] A. Kathiravan, G. Paramaguru, R. Renganathan, Study on the binding of colloidal zinc oxide nanoparticles with bovine serum albumin, J. Molecular Struct. 934(1-3) (2009) 129-137.

[22] S. Chakraborty, P. Joshi, V. Shanker, Z.A. Ansari, S.P. Singh, P. Chakrabarti, Contrasting effect of gold nanoparticles and nanorods with different surface modifications on the structure and activity of bovine serum albumin, Langmuir 27(12) (2011) 7722-7731.

[23] Z. Nasir, M. Shakir, R. Wahab, M. Shoeb, P. Alam, et al., Co-precipitation synthesis and characterization of Co doped SnO_2 NPs, HSA interaction via various spectroscopic techniques and their antimicrobial and photocatalytic activities, Int. J. Biol. Macromol. 94 (2017) 554-565.

[24] S. Millan, A. Kumar, L. Satish, B. Susrisweta, P. Dash, H. Sahoo, Insights into the binding interaction between copper ferrite nanoparticles and bovine serum albumin: An effect on protein conformation and activity, Luminescence 33(6) (2018) 990-998.

[25] S. Chakraborti, P. Joshi, D. Chakravarty, V. Shanker, Z.A. Ansari, et al., Interaction of polyethyleneimine-functionalized ZnO nanoparticles with bovine serum albumin, Langmuir 28(30) (2012) 11142-11152.

https://doi.org/10.30799/jnst.242.19050409

Cite this Article as: Neelam, Mahima Kaushik, Physicochemical interactions of APTS-$ZnFe_2O_4$ nanoparticles with bovine serum albumin (BSA): Biomedical applications, J. Nanosci. Tech. 5(4) (2019) 776–779.